Lysinibacillus fusiformis M5 induces increased complexity in *Bacillus subtilis* 168 colony biofilms via hypoxanthine

Ramses Gallegos-Monterrosa[1], Stefanie Kankel[1], Sebastian Götze[2], Robert Barnett[2], Pierre Stallforth[2,*], Ákos T. Kovács[1,*,#]

[1] Terrestrial Biofilms Group, Institute of Microbiology, Friedrich Schiller University Jena, Jena, Germany.

[2] Junior Research Group Chemistry of Microbial Communication, Leibniz Institute for Natural Product Research and Infection Biology, Hans Knöll Institute – HKI, Jena, Germany.

Running Title: *L. fusiformis* M5 interaction with *B. subtilis* 168

* Address correspondence to: Ákos T. Kovács <atkovacs@dtu.dk> (on microbiology and strain requests) or Pierre Stallforth < pierre.stallforth@leibniz-hki.de> (on isolation and identification of metabolites)

[#] Affiliation from July 1st 2017: Department of Biotechnology and Biomedicine, Technical University of Denmark, Denmark

ABSTRACT

In recent years, biofilms have become a central subject of research in the fields of microbiology, medicine, agriculture, or systems biology amongst others. The sociomicrobiology of multispecies biofilms, however, is still poorly understood. Here, we report a screening system that allowed us to identify soil bacteria, which induce architectural changes in biofilm colonies when cocultured with *B. subtilis*. We identified the soil bacterium *Lysinibacillus fusiformis* M5 as inducer of wrinkle-formation in *B. subtilis* colonies mediated by a diffusible signaling molecule. This compound was isolated by bioassay-guided chromatographic fractionation. The elicitor was identified to be the purine hypoxanthine using mass spectrometry and nuclear magnetic resonance (NMR) spectroscopy. We show that the induction of wrinkle formation by hypoxanthine is not dependent on signal recognition by the histidine kinases KinA, KinB, KinC, and KinD, which are generally involved in phosphorylation of the master regulator Spo0A. Likewise, we show that hypoxanthine signaling does not induce the expression of biofilm-matrix related operons *epsA-O* and *tasA-sipW-tapA*. Finally, we demonstrate that the purine permease PbuO, but not PbuG, is necessary for hypoxanthine to induce an increase in wrinkleality of *B. subtilis* biofilm colonies. Our results suggest that hypoxanthine-stimulated wrinkle development is not due to a direct induction of biofilm-related gene expression, but rather caused by the metabolic changes derived from the excess of hypoxanthine in *B. subtilis* cells.

41 **IMPORTANCE**

42 Biofilms are a bacterial lifestyle with high relevance regarding diverse human activities.
43 Biofilms can be favorable, for instance in crop protection. In nature, biofilms are
44 commonly found as multispecies communities displaying complex social behaviors and
45 characteristics. The study of interspecies interactions will thus lead to a better
46 understanding and use of biofilms as they occur outside laboratory conditions. Here, we
47 present a screening method suitable for the identification of multispecies interactions,
48 and showcase *L. fusiformis* as a soil bacterium that is able to live alongside *B. subtilis*
49 and modify the architecture of its biofilms.

INTRODUCTION

Biofilms are microbial populations formed by cells living in high density communities attached to biotic or abiotic surfaces. These cells are often encased in a matrix of polymeric substances that provide the whole population with an increased resistance against environmental stress (1, 2). Furthermore, these communities exhibit highly complex structural organization and social behavior. Thus, biofilms have become an increasingly studied research subject by microbiologists, especially when it became apparent that this lifestyle is widely spread among bacteria and involved in a multitude of biological processes (3, 4). Although much attention has been given to medically-relevant biofilms (5, 6), scientists have also studied biofilms in the context of industrial applications (7), bioremediation (8), and crop protection (9).

In nature, biofilms rarely occur as single-species populations, but rather as mixed communities of diverse bacteria and other microorganisms. This leads to complex interactions between the different members of the community, usually involving communication networks based on chemical signals (10). Additionally, microorganisms need to sense and efficiently adapt to a wide array of environmental cues in order to efficiently regulate biofilm formation (11).

Bacillus subtilis is a soil-dwelling Gram-positive bacterium that has become a model for biofilm research. On agar plates, *B. subtilis* can form large colonies with remarkably complex architecture, while in liquid medium it forms robust floating biofilms known as pellicles. Both forms of biofilms are characterized by a wrinkled surface, which has been associated to the production of exopolysaccharides, biofilm maturation, and mechanical

74 forces concomitant with an increased population complexity (12–14). Moreover, these
75 biofilms display intricate cell heterogeneity, i.e. some cells become matrix producers,
76 while others either produce exoenzymes to harvest nutrients, or form resistant structures
77 known as spores (15, 16). The development of this population heterogeneity is regulated
78 by a complex gene regulatory network involving various sensing kinases i.e. Kin
79 kinases, DegS, and ComP and their concomitant response regulators Spo0A, DegU,
80 and ComA (15, 17), respectively.
81
82 Biofilms produced by *B. subtilis* are not only a good research model, they are currently
83 applied in crop protection (18, 19), and spores of this organism are readily
84 commercialized as a biocontrol agent for agriculture. *B. subtilis* is a prolific producer of
85 secondary metabolites and many potent antimicrobial compounds inhibiting both
86 bacteria and fungi have been identified (20–22). In addition, it has also been shown that
87 *B. subtilis* activates biofilm-related gene expression in response to chemicals produced
88 by other bacteria closely related to it, for instance by other members of the *Bacillus*
89 genus (23). Interestingly, the signaling role of the molecules can be independent from
90 other effects of the compounds, as in the case of antimicrobial thiazolyl peptides, which
91 can induce biofilm-matrix production in *B. subtilis* even when separated from their
92 antibiotic activity (24). Moreover, other organisms such as *Pseudomonas protegens*, are
93 able to inhibit cell differentiation and biofilm gene expression in *B. subtilis*, possibly as a
94 competition strategy during root colonization (25).
95
96 *B. subtilis* successfully inhabits a congested and competitive ecological niche (26–28),
97 and it is to be expected that this organism has a finely tuned regulatory network

98 governing community behavior. Therefore, further study of the signaling mechanisms
99 that influence *B. subtilis* biofilm formation may enhance the use of this organism, both in
100 biotechnological applications as well as a research model. However, the identification of
101 signals that induce biofilm formation is a poorly investigated field of study, possibly due
102 to the greater general interest in the removal of biofilms in various medical and industrial
103 settings (5, 29–31). Thus, we have established a co-cultivation-based screening method
104 to identify signaling molecules that induce biofilm formation in *B. subtilis*. Using this
105 system, we identified ecologically relevant soil bacteria that are able to induce the
106 formation of large wrinkles in colony biofilms of *B. subtilis*. The majority of these bacteria
107 are members of the family *Bacillaceae*, to which *B. subtilis* belongs. The strain with the
108 clearest wrinkle-inducing effect was identified as *Lysinibacillus fusiformis* M5. The
109 observed effect on *B. subtilis* is dependent on a diffusible signaling molecule, which was
110 identified as hypoxanthine using bioassay-guided fractionation and subsequent structure
111 elucidation using various spectroscopic and spectrometric methods. The induction of
112 wrinkles by hypoxanthine was not dependent on Kin kinases signal transduction, and
113 the expression levels of operons responsible for the production of biofilm matrix
114 components, *epsA-O* and *tapA-sipW-tasA*, remained unaffected. We show that uptake
115 of hypoxanthine by permease PbuO is necessary for the increased wrinkleality of *B.*
116 *subtilis* biofilms colonies, where wrinkleality refers to the degree of wrinkle formation as
117 defined by Spiers (32). We therefore suggest that hypoxanthine induces the formation of
118 wrinkles by introducing a metabolic change in *B. subtilis* cells, rather than by direct
119 stimulation of biofilm-related gene expression.

RESULTS

Screening of soil bacteria that induce structural changes in colonies of *B. subtilis.*

We screened a collection of 242 strains isolated from two distinct soil sampling sites in Mexico, in order to identify bacteria that are able to induce biofilm formation or increased complex colony architecture of *B. subtilis*. Importantly, our assay aimed to discover alterations in biofilm colony architecture that was different from the previously described method that identified soil-derived microbes that induce gene expression related to biofilm formation of *B. subtilis* (23). While some *B. subtilis* strains, such as *B. subtilis* NCIB 3610, easily and spontaneously form biofilms, we used a strain that would form architecturally complex colonies only in the presence of specific inducers or nutrient rich conditions. Thus, even weak biofilm-inducing effects would not be overseen. We used *B. subtilis* 168 (Jena stock), a strain that can only form architecturally complex colonies when grown on glucose-rich medium or exposed to signaling molecules as present in plant root exudates (33). The strain of *B. subtilis* used for the assay (TB48) carried a $P_{hyperspank}$-mKATE reporter fusion in order to facilitate the identification of *B. subtilis* from the soil strains in mixed colonies. The reporter strain was mixed in different ratios with the bacterial isolates and allowed to form colonies on 2×SG medium for 72 hours. Single strain colonies of *B. subtilis* and the soil-derived isolates were also grown as neighboring colonies under the same conditions, inoculated with a spatial distance of 5 mm between each other to examine their interactions. The majority of these interactions resulted in the apparent killing of one strain by the other, producing a colony identical to the pure culture colony of the surviving partner (data not shown). However, 36 soil strains were able to grow alongside *B. subtilis*, mainly by creating a colony where the strains segregate in sectors. Interestingly, the *B. subtilis* sectors of these mixed colonies

144 showed a marked increase in the formation of wrinkles compared to its pure colonies
145 (Fig. 1). Furthermore, when single strain colonies of these soil-derived isolates were
146 grown close to *B. subtilis* colonies, the induction of wrinkle formation could be observed
147 in the areas of the *B. subtilis* colony that are closest to the soil strain, but not in the other
148 regions of the colony (Fig. 1). These results suggest that the aforementioned bacteria
149 produce signals that can induce an increased architectural complexity in *B. subtilis*
150 colony biofilms.
151

152 **Structural changes in *B. subtilis* colonies are induced by diffusible signals**
153 **produced by soil bacteria.**

154 In order to elucidate if the observed induction of wrinkle formation is caused by a
155 diffusible signal molecule or due to direct cell-cell interactions, we designed an assay to
156 test the cell-free supernatants of the selected soil strains. In this assay, we used cotton
157 discs infused with cell-free supernatant to simulate colonies of the tested soil strains.
158 *B. subtilis* was inoculated at a distance of 5 mm next to the cotton discs and allowed to
159 grow for 72 hours. Over this period, the growing colony surrounded the cotton discs,
160 getting into contact with the freely diffusing compounds in the supernatants.
161 Using this assay, we observed that the cell-free supernatants of four bacterial isolates
162 were able to induce efficiently the formation of wrinkles in the adjacent *B. subtilis* colony.
163 Importantly, this phenomenon was observed in the periphery of the cotton discs, but not
164 in the areas of the colony farther away from it (Fig. 2). We note that neither the cell-free
165 supernatant of *B. subtilis* itself nor the medium used to obtain the supernatants showed
166 the capacity to induce increased wrinkleality in *B. subtilis* colonies under our tested

conditions (Fig. 2). We concluded that the induction of wrinkle formation was due to a diffusible signaling molecule produced by these soil organisms.

Using 16S rRNA locus sequencing, we characterized those soil strains whose supernatant could best stimulate wrinkle formation in *B. subtilis*. The majority of the sequenced strains were found to be members of the same phylogenetic family as *B. subtilis*, such as *Bacillus pumilus* or *L. fusiformis*. The only exception was a strain identified as the γ-proteobacterium *Acinetobacter variabilis.*

Hypoxanthine was identified in the supernatant to be responsible for wrinkle induction.

The clearest and strongest induction of wrinkle formation was observed in the supernatant of the soil derived strain identified as *L. fusiformis* M5. For this reason, we decided to further investigate the respective signaling molecule produced by this bacterium using a colony wrinkleality assay. Bio-assay-guided fractionation allowed then to identify a compound from *L. fusiformis* M5 that induced a similar phenotype as observed when *B. subtilis* and *L. fusiformis* M5 were co-cultured. To this end, supernatant of *L. fusiformis* M5 was lyophilized and fractionated using Sephadex G20 as stationary phase. Each fraction was applied to cotton discs and placed on an agar plate in the vicinity of *B. subtilis.* The fraction that induced wrinkle formation was sub-fractionated by high-performance liquid chromatography (HPLC) using a hypercarb column as stationary phase. Repeating this procedure led to the isolation of a homogeneous compound whose structure was subsequently elucidated via a combination of nuclear magnetic resonance (NMR) spectroscopy and high-resolution mass spectrometry (HR-MS). Finally, hypoxanthine was identified as the inducer of

191 wrinkle formation. We further validated our findings using commercial hypoxanthine,
192 which showed the same properties as the isolated hypoxanthine (Fig. 3).
193
194 **Hypoxanthine signaling is not mediated by Kin kinases**
195 In *B. subtilis*, the transcriptional regulator Spo0A controls the expression of several
196 biofilm-related operons, including those responsible for the production of the
197 exopolysaccharide and protein components of the biofilm matrix (*epsA-O* and *tapA-*
198 *sipW-tasA*, respectively) (17). Five sensor kinases (KinA, KinB, KinC, KinD, and KinE)
199 have been identified in *B. subtilis*, while four of them (KinA-D) are known to activate
200 Spo0A via a phosphorelay depending on the environmental signals (11, 15, 34). We
201 wanted to determine if any of these kinases is involved in hypoxanthine-mediated
202 induction of wrinkles. Therefore, we compared the effect that the supernatant of *L.*
203 *fusiformis* M5 has on kinase-mutant strains of *B. subtilis* using our colony wrinkleality
204 assay. We expected that, should one of these kinases be responsible for sensing
205 hypoxanthine, the corresponding mutant strain would no longer show increased colony
206 wrinkleality. Interestingly, all the mutant strains were still able to develop highly wrinkled
207 colonies when exposed to the supernatant (Fig. 4). This result indicates that
208 hypoxanthine-mediated induction of increased architectural complexity is not mediated
209 by the activation of Spo0A via the Kin kinases.
210
211 **Expression levels of genes responsible for biofilm matrix production are not**
212 **affected by hypoxanthine signaling.**
213 The *epsA-O* and *tapA-sipW-tasA* operons are related to the production of the
214 exopolysaccharide and protein components of the *B. subtilis* biofilm matrix, respectively.

215 Changes in the expression levels of these operons are associated to a maturating
216 biofilm, and show spatiotemporal variation during its development (16, 35, 36).
217 To further examine if biofilm matrix-related genes are involved in the induction of
218 wrinkles by hypoxanthine, we monitored the expression of P_{epsA}-*gfp* and P_{tapA}-*gfp*
219 fluorescent reporter fusions in colonies of *B. subtilis* using our colony wrinkleality assay.
220 Fluorescence emission was examined only in the sections of the colonies directly
221 adjacent to the cotton discs at 3 time points: (i) when *B. subtilis* has encircled the discs
222 (40 hours), (ii) when the colony started to expand from the disc and showed the onset of
223 wrinkle formation (50 hours), and (iii) when the colony has developed wrinkles and
224 expanded (65 hours). The examined strains also carried a $P_{hyperspank}$-*mKATE* reporter
225 fusion to adjust for colony growth. Under these conditions, the expression from P_{epsA} and
226 P_{tapA} in these colonies showed no statistical differences when exposed to cotton discs
227 infused with 2×SG medium or supernatant of *B. subtilis,* as compared to those infused
228 with supernatant of *L. fusiformis* M5 (one-way ANOVA: $P<0.05$, n=4-8 independent
229 colonies) (Fig. 5).
230 Taken together, these results suggest that the increased colony wrinkleality induced by
231 hypoxanthine is not directly associated to biofilm matrix-related gene expression.
232

233 **The permease PbuO is necessary for hypoxanthine-induced development of**
234 **wrinkles.**

235 We hypothesized that the observed induction of wrinkle formation may be due to
236 metabolic effects on *B. subtilis* cells derived from an excess of available hypoxanthine
237 provided by the culture supernatant of *L. fusiformis* M5, rather than to direct signal-
238 dependent expression of biofilm-related genes. In this case, hypoxanthine alone would

239 be sufficient to induce increased wrinkleality, and its uptake by *B. subtilis* would be
240 necessary for this phenomenon.
241 Different concentrations of hypoxanthine (as solution in 0.05 N NaOH) were able to
242 induce the formation of wrinkles in *B. subtilis* colonies as efficiently as the supernatant of
243 *L. fusiformis* M5. To test whether hypoxanthine internalization is required for the
244 observed wrinkle induction in *B. subtilis*, we analyzed mutant strains of *B. subtilis* that
245 lack *pbuG* or *pbuO*. PbuG is a previously described hypoxanthine/guanine permease
246 (37), while PbuO is a protein paralogous to PbuG annotated as a putative purine
247 permease (see SubtiWiki: http://subtiwiki.uni-goettingen.de/index.php). These strains
248 were studied with our colony wrinkleality assay. The hypoxanthine inducing effect
249 disappeared when *pbuO* alone, or in combination with *pbuG,* was deleted (Fig. 6).
250 These final results demonstrated that hypoxanthine uptake is important for induction of
251 wrinkle formation and PbuO is mainly responsible for the observed effect under our
252 experimental conditions.

253 **DISCUSSION**

254 In this work, we identified a chemical sensing mechanism between *B. subtilis* and other
255 soil bacteria that promotes architectural complexity in colony biofilms. We devised a
256 screening system that allowed us to analyze a collection of soil bacteria, selecting those
257 that could form stable multispecies communities with *B. subtilis*. Using this screening
258 system, we identified *L. fusiformis* M5 as a bacterium inducing an increase of colony
259 wrinkleality in *B. subtilis* via hypoxanthine as chemical cue.

260

261 Hypoxanthine is a purine that plays an important role in the pentose phosphate salvage
262 pathway, which is a mechanism for cells to interconvert nucleosides and nucleobases
263 according to their metabolic needs (38, 39). In *B. subtilis*, hypoxanthine is particularly
264 relevant in this pathway because it can be taken up by cells and used as a substrate by
265 phosphoribosyl-transferases in order to produce inosine monophosphate (IMP), which in
266 turn is converted to adenosine monophosphate or guanine monophosphate (37) (also
267 see SubtiWiki Pathways: http://subtiwiki.uni-
268 goettingen.de/apps/pathway.php?pathway=2). The role of hypoxanthine in eukaryotic
269 cell metabolism has been extensively investigated. In humans, it has been studied in the
270 context of diseases such as gout, Lesch–Nyhan disease, and endothelial cell injury of
271 cardiovascular diseases. Although these conditions have different etiologies and clinical
272 evolution, they have in common an excessive accumulation of hypoxanthine and uric
273 acid that leads to oxidative-stress-induced apoptosis (40–42). In bacteria, hypoxanthine
274 has been mainly studied in relation to DNA damage and mutagenesis due to
275 spontaneous deamination of adenine, which yields hypoxanthine and leads to AT-to-GC
276 transitions after DNA replication (43). In *B. subtilis*, hypoxanthine has been studied both

277 related to purine metabolism (37), and DNA damage and repair (44). To the best of our
278 knowledge, this is the first time that hypoxanthine has been reported as a mediator of
279 interactions in *B. subtilis* biofilms.
280
281 *L. fusiformis* is a free-living bacterium that can be isolated from soil and has been
282 studied due to its production of interesting secondary metabolites and bioremediation
283 potential (45–47). Here, we have identified a strain of *L. fusiformis* able to produce and
284 excrete hypoxanthine in sufficient levels to induce the formation of wrinkles in biofilm
285 colonies of *B. subtilis*. We found no evidence that this phenomenon is dependent on Kin
286 kinases signal transduction, and the expression levels of the matrix-component-related
287 operons *epsA-O* and *tapA-sipW-tasA* remained equal when *B. subtilis* was exposed to
288 the supernatant of *L. fusiformis* M5. However, a knock-out mutant of the
289 hypoxanthine/guanine permease, PbuO, lost the ability to form heavily wrinkled colonies.
290 A *pbuG*$^{-}$ mutant strain showed comparable or in rare cases slightly reduced wrinkle
291 formation, while a *pbuO*$^{-}$ strain completely lost the ability to form wrinkled colonies when
292 exposed to hypoxanthine. Based on these results, we conclude that hypoxanthine
293 induces the formation of wrinkles in colony biofilms of *B. subtilis* not by inducing the
294 expression of biofilm-related genes, but rather by metabolic effects derived from the
295 excess of available hypoxanthine. In this regard, we note that an excess of hypoxanthine
296 can cause oxidative stress and cell death in eukaryotic cells (40, 41), while localized cell
297 death can lead to the formation of wrinkles in colonies of *B. subtilis* by providing an
298 outlet for mechanical forces that shape the developing biofilm (13). Thus, we
299 hypothesize that the hypoxanthine provided by *L. fusiformis* induces cell stress and
300 possibly cell death in *B. subtilis*, which leads to the formation of wrinkles as a

301 mechanical consequence. This is in accordance with the fact that the observed
302 development of wrinkles only occurs in the interaction zone between colonies of these
303 organisms (Fig. 1), or in the proximity of the cotton discs during our colony wrinkleality
304 assays (Figs. 4 and 6). This development of wrinkles does not happen in the rest of the
305 *B. subtilis* colony, presumably due to a lower concentration of diffused hypoxanthine.
306 Importantly, this induction of increased wrinkleality in *B. subtilis* may be a consequence
307 of regular metabolic processes of *L. fusiformis*, rather than a canonical signaling
308 mechanism intended to elicit a response in the receiver. Regarding hypoxanthine
309 production by *L. fusiformis* M5, we have previously sequenced this strain, finding genes
310 homologous to those known in other organisms to be responsible for hypoxanthine
311 synthesis and export (48), although more research is needed to establish its production
312 yield. However, we note that hypoxanthine can be produced by spontaneous
313 deamination of adenine, such as that present in the surroundings of decaying cells (49).
314 Unfortunately, our efforts to transform *L. fusiformis* M5 failed, preventing us to construct
315 mutants with altered hypoxanthine production.
316
317 In recent years, biofilm research has grown from an incipient field to a major area of
318 microbiological interest. Due to the high cell density of biofilms, social interactions are an
319 inherent characteristic of these microbial populations, regardless of whether they are
320 formed as single or multi-species communities (10, 27, 50, 51). The interactions
321 between the organisms forming a biofilm are therefore an important aspect of this
322 research field, since they shape the development of these communities, be it by
323 intraspecies signaling, interspecies communications, or chemical cues derived from the
324 metabolism of community members, such as the case presented here. Further study of

325 the sociomicrobiology of biofilms will lead to an increased understanding of these
326 communities as they form in nature, better enabling us to eliminate them when they are
327 noxious to human activities, or to promote them when needed for biotechnological
328 applications.

329 **MATERIAL AND METHODS**

330 **Strains, media, and general culture conditions.**

331 All strains used in this study are listed in Table 1. When fresh cultures were needed,
332 these strains were pre-grown overnight in Lysogeny broth medium (LB-Lennox, Carl
333 Roth; 10 g L^{-1} tryptone, 5 g L^{-1} yeast extract, and 5 g L^{-1} NaCl) at 37°C and shaken at
334 225 r.p.m. LB medium was used for all *B. subtilis* and *Escherichia coli* transformations,
335 and to screen soil samples. 2×SG medium (16 g L^{-1} nutrient broth (Difco), 2 g L^{-1} KCl,
336 0.5 g L^{-1} $MgSO_4 \cdot 7H_2O$, 1mM $Ca(NO_3)_2$, 0.1mM $MnCl_2 \cdot 4H_2O$, 1 µM $FeSO_4$, and 0.1%
337 glucose) (52) was used to grow cultures intended for supernatant production. This
338 medium was also used for all strain interaction assays and wrinkle-induction assays.
339 Tryptone Soya broth (CASO-Bouillon, AppliChem; 2.5 g L^{-1} glucose, 5 g L^{-1} NaCl, 2.5 g
340 L^{-1} buffers (pH 7.3), 3 g L^{-1} soya peptone, and 17 g L^{-1} tryptone) was used for screening
341 soil samples. GCHE medium (1% glucose, 0.2% glutamate, 100mM potassium
342 phosphate buffer (pH: 7), 3mM trisodium citrate, 3mM $MgSO_4$, 22 mg L^{-1} ferric
343 ammonium citrate, 50 mg L^{-1} L-tryptophan, and 0.1% casein hydrolysate) was used to
344 induce natural competence in *B. subtilis* (53). Our developed Gallegos Rich medium was
345 used to grow *Lactococcus lactis* MG1363, in order to purify pMH66: 21 g L^{-1} tryptone, 5
346 g L^{-1} yeast extract, 8.3 g L^{-1} NaCl, 3 g L^{-1} soya peptone, 2.6 g L^{-1} glucose, and 2.5 g L^{-1}
347 $MgSO_4 \cdot 7H_2O$. Overnight cultures of *L. lactis* were incubated at 30°C without shaking.
348 Media were supplemented with Bacto agar 1.5 % when solid plates were needed.
349 Antibiotics were used at the following final concentrations: kanamycin, 10 µg mL^{-1};
350 chloramphenicol, 5 µg mL^{-1}; erythromycin-lincomycin, 0.5 µg mL^{-1} and 12.5 µg mL^{-1}
351 respectively; ampicillin, 100 µg mL^{-1}; spectinomycin, 100 µg mL^{-1}; tetracycline, 10 µg
352 mL^{-1}. Specific growth conditions are described in the corresponding methods section.

353

354 Importantly, all 2×SG plates used in this study were prepared with 25 mL of medium,
355 and dried for a minimum of 20 minutes before use. Insufficient drying resulted in
356 excessive colony expansion without development of architecturally complex colonies. To
357 dry the plates, they were first allowed to solidify at room temperature for 1 hour,
358 afterwards, they were kept completely open in a laminar flow sterile bench for the
359 duration of the drying period. These drying conditions were followed for all assays that
360 examined changes in colony architecture.

361

362 **Strain construction.**

363 All *B. subtilis* strains generated in this work were obtained via natural competence
364 transformation (53) using genomic or plasmid DNA from donor strains as indicated in
365 Table 1. Briefly, overnight cultures of the receiver strains were diluted to a 1:50 ratio with
366 GCHE medium, these cultures were incubated at 37°C for 4 h with shaking at 225 r.p.m.
367 After this incubation period, 5–10 µg of genomic or plasmid DNA were mixed with 500
368 µL of competent cells and further incubated for 2h before plating on LB plates added
369 with selection antibiotics. Strain TB822 was obtained by using the Cre recombinase
370 expressed from plasmid pMH66 to eliminate the Erm^R cassette of TB813, and
371 subsequently curating pMH66 via thermal loss of the plasmid (54). Briefly, TB813 was
372 transformed with 10 µg of pMH66, selecting transformants via incubation at 37°C on LB
373 plates added with tetracycline. Candidates were then screened for their capacity to grow
374 at 37°C on LB plates added with macrolide antibiotics (erythromycin-lincomycin), those
375 that were not able to grow were further incubated on LB plates at 43°C for 18 h to induce

376 the loss of pMH66. Candidates that were then unable to grow at 37°C on LB plates
377 added with tetracycline were considered to have lost pMH66.
378 Successful construction of all used strains and plasmids was validated via PCR and
379 restriction pattern analysis using standard molecular biology techniques. All PCR
380 primers used in this study are listed in Table 2. Primer pairs were used to amplify the
381 indicated loci (see Table 2), in order to confirm the proper mutation of the corresponding
382 gene. To confirm the correct construction of strains TB869 and TB870, primer oGFPrev2
383 was used in combination with oRGM38 (for *sacA*::P_{tapA}-*gfp*) or oRGM40 (for *sacA*::P_{epsA}-
384 *gfp*).
385
386 **Isolation of bacteria from soil samples.**
387 Two independent Mexican soil samples were screened to isolate bacteria able to grow
388 on LB or tryptone soya broth media. The first sample was collected from Tepoztlán,
389 Morelos (18° 59′ 7″ N, 99° 5′ 59″ W), a humid and verdant region of central Mexico. The
390 second sample was collected from Tehuacán, Puebla (18° 25′ 47.71″ N, 97° 27′ 58.1″
391 W), a semidesertic dry region in east central Mexico. Both samples were collected with a
392 clean metal spatula 5 cm below surface level, and at 15 to 20 cm of the roots of local
393 trees.
394
395 1 g of each soil sample was suspended in 9 mL of a sterile 0.85% NaCl solution, and 50
396 µL of Tween 80 were added. The resulting suspensions were vortexed for 5 minutes at
397 maximum speed. The bigger soil particles were allowed to sediment by keeping the
398 suspensions still for 10 minutes. The supernatants were then diluted with sterile 0.85%
399 NaCl to 1:1000, 1:10 000 and 1:100 000 ratios. 50 and 100 µL of these dilutions were

400 spread on LB and tryptone soya broth agar plates. These plates were incubated at 30°C
401 for a maximum of 5 days. Bacterial colonies that grew during the incubation period were
402 further isolated by cross-streaking them on LB or tryptone soya broth plates and
403 incubating them at 30°C for 48 hours. Single isolated colonies obtained from this
404 secondary cultivation were used to prepare liquid cultures on 3 mL of LB media. These
405 cultures were incubated at 30°C with shaking for a maximum of 48 hours. Bacteria that
406 grew efficiently during this incubation period were used to prepare glycerol stock
407 solutions (20% v/v) and stored at -80°C for further use. In total, 242 soil strains were
408 obtained and subsequently tested.
409
410 **Soil strains interaction screening.**
411 Overnight liquid cultures of *B. subtilis* strain TB48 and the obtained soil strains were
412 adjusted to OD_{600} 0.2 using LB medium. These diluted cultures were then mixed in 1:1,
413 10:1, and 1:10 ratios, and 2 µL of the mixed and pure cultures were inoculated on 2×SG
414 plates. For neighbor colonies interaction assay, 2 µL of the pure cultures were
415 inoculated at a distance of 5 mm from each other. Plates were incubated at 30°C for 72
416 h. The obtained colonies were used for microscopy analysis without further treatment.
417
418 **Identification of soil strains.**
419 Genomic DNA of selected soil strains was extracted with the GeneMATRIX Bacterial
420 and Yeast Genomic DNA Purification Kit, according to the manufacturer's instructions
421 (EURx, Poland). This DNA was used to PCR amplify a fragment of the 16S rRNA gene
422 using primers 27F and 1492R (55). Amplicons were purified with the High Pure PCR
423 Product Purification Kit according to the manufacturer's instructions (Roche Diagnostics,

424 Switzerland) and sequenced with primers 27F and 1492R (GATC Biotech, Germany).
425 Sequencing results were then compared with sequences in the National Center for
426 Biotechnology Information (16S ribosomal RNA Bacteria and Archaea database) using
427 the BLASTn algorithm (56). Soil strains' identities were established using minimum
428 query coverage of 98% and minimum identity values of 99%.
429
430 **Purification and treatment conditions of soil strain supernatant.**
431 To obtain cell-free supernatants of selected soil strains, 10 mL cultures on 2×SG
432 medium of the corresponding strains were incubated at 30°C for 24 hours with shaking
433 at 100 r.p.m. These cultures were then centrifuged at 7000 r.c.f. for 15 min. The
434 supernatants were collected and filter-sterilized using a 0.22 µm pore-size filter (Carl
435 Roth, Germany).
436
437 **Colony wrinkleality assay.**
438 We developed the following assay to assess the effect that the supernatants of soil
439 strains, and compound solutions, may have upon the architectural complexity of *B.*
440 *subtilis* colony biofilms. Sterile 12 mm-diameter cotton discs were placed on 90 mm-
441 diameter 2×SG agar plates, in such a way that there is a maximum amount of available
442 space among the discs themselves and between the discs and the border of the plates.
443 3 cotton discs were used per plate. 50 µL of the tested supernatant or compound
444 solution were deposited on the center of the cotton discs, and the plates were dried for 3
445 min by keeping them completely open in a laminar flow sterile bench. This drying period
446 was done in addition to the regular 20 min drying previously described. 2 µL of an
447 overnight culture of the tested strains were then inoculated at 5 mm from the edge of the

448 cotton discs. The plates were incubated at 30°C for a total of 72 hours. Every 24 hours
449 the cotton discs were reimpregnated with 25 µL of the corresponding supernatant or
450 compound solution. After the incubation period, the plates were used for microscopy
451 analysis without further treatment.
452
453 **Bioassay-guided fractionation.**
454 A 50 mL culture of M5 isolate was grown for 24 h under standard conditions. Bacterial
455 cells were pelleted by centrifugation for 10 min at 6.000 *g* and the supernatant was
456 filtered through a 0.2 µm filter. 25 mL of the supernatant were freeze-dried and the
457 remaining foam was dissolved in 1 mL water. The solution was applied to a Sephadex
458 G20 column (3 cm × 40 cm) and eluted with water collecting 3 mL fractions (50
459 fractions). Fractions were further analyzed using the colony wrinkleality assay. The
460 fraction with the largest activity was analyzed using an LCMS (Shimadzu Deutschland,
461 Germany) equipped with a Hypercarb column (100 × 3 mm, 3 µM, Thermo Fisher
462 Scientific, flow rate = 0.6 mL min^{-1}, method: 0-10 min: 100% (v/v) water). The main
463 compound of this fraction was purified using a semi-preparative HPLC (Shimadzu
464 Deutschland, Germany) equipped with Hypercarb column (100 × 10 mm, 5 µM, Thermo
465 Fisher Scientific, flow rate = 5 mL min^{-1}, method = 0-20 min: 100% (v/v) water). The pure
466 compound was analyzed using ^{1}H-NMR spectroscopy, LCMS, and HR-ESIMS. Obtained
467 analytical data were in good agreement with a hypoxanthine standard from Sigma
468 Aldrich.
469
470 **Comparison of hypoxanthine production.**

471 Supernatant of different isolates were heated to 80°C for 15 min and filtered through a
472 0.2 µm syringe filter. The samples were analyzed using an LCMS (Shimadzu
473 Deutschland, Germany) equipped with a Hypercarb column (100 × 3 mm, 3 µM, Thermo
474 Fisher Scientific, flow rate = 0.6 mL min^{-1}, method: 0-10 min: 100% (v/v) water).
475
476 **Stereomicroscopy and Image Analysis.**
477 All bright-field and fluorescence images of colonies were obtained with an Axio Zoom
478 V16 stereomicroscope (Carl Zeiss, Germany) equipped with a Zeiss CL 9000 LED light
479 source, a PlanApo Z 0.5× objective, HE 38 eGFP filter set (excitation at 470/40 nm and
480 emission at 525/50 nm), HE 63 mRFP filter set (excitation at 572/25 nm and emission at
481 629/62 nm), and AxioCam MRm monochrome camera (Carl Zeiss, Germany).
482
483 Images were obtained with exposure times of 20 ms for bright-field, and 2500 ms for red
484 fluorescence or 3000 ms for green fluorescence when needed. For clarity purposes, the
485 images of colonies are presented here with adjusted contrast and the background has
486 been removed, so that the colony structures can be easily appreciated. The modified
487 pictures were not used for any fluorescence measurements.
488
489 To assess the expression levels of P_{epsA}-*gfp*, P_{tapA}-*gfp,* and $P_{hyperspank}$-*mKATE*
490 fluorescent reporter fusions in colonies we used ImageJ (National Institutes of Health,
491 USA). Briefly, the average fluorescence emission intensities were measured in the green
492 fluorescence channel for GFP and red fluorescence channel for mKATE by using a
493 region of interest (ROI) that surrounds the cotton discs in the pictures as a partial ring,
494 taking care to avoid the disc area itself. The ROI was drawn in such a way that it avoids

495 the region of the colony that first makes contact with the cotton discs. This ROI had a
496 width of 0.5 mm for measurements done at 40 and 50 hours, and a width of 1 mm for
497 measurements done at 65 hours. The ROI was positioned in each colony image using
498 the bright-field channel, and the average fluorescence intensity was then measured on
499 the corresponding green and red fluorescence images.
500
501 **Nucleotide sequence accession numbers.**
502 Sequences used in this study have been deposited in GenBank under accession
503 numbers KY705015 (*Lysinibacillus* sp. M2c), KY698015 (*Bacillus pumilus* P22a), and
504 KY703395 (*Acinetobacter variabilis* T7a). Further, the draft genome sequence of *L.*
505 *fusiformis* M5 is available in GenBank under accession number MECQ00000000, and
506 the strain was deposited in the Jena Microbial Resource Collection (ST-Number:
507 ST036146, see http://www.leibniz-hki.de/en/jena-microbial-resource-collection.html).

508 **AUTHORS CONTRIBUTIONS**

509 R.G.-M., Á.T.K. conceived the project; R.G.-M., S.K. performed the screen and the
510 microbiology assays; R.G.-M. constructed bacterial strains; S.G., purified hypoxanthine;
511 S.G., R.B., P.S. analyzed the analytical data; R.G.-M., P.S., Á.T.K., wrote and revised
512 the manuscript.

513

514 **ACKNOWLEDGEMENTS**

515 We would like to thank Heike Heineke (HKI Jena) for NMR measurements and Andrea
516 Perner (HKI Jena) for HR-MS measurements.
517 Ákos T. Kovács was funded by a Marie Curie Career Integration Grant
518 (PheHetBacBiofilm), Deutsche Forschungsgemeinschaft (DFG) (KO4741/2-1 and
519 KO4741/3-1), and DFG Graduate School Jena School of Microbial Communication
520 (JSMC) (Start-up Grant). Ramses Gallegos-Monterrosa was funded by Consejo
521 Nacional de Ciencia y Tecnología, German Academic Exchange Service. Sebastian
522 Götze, Robert Barnett, and Pierre Stallforth was funded by Leibniz Association (Junior
523 Research Group of Pierre Stallforth). Robert Barnett was funded by DFG Graduate
524 School Jena School of Microbial Communication (JSMC) (PhD fellowship to Robert
525 Barnett).

526

527 **REFERENCES**

528 1. **Hall-Stoodley L, Costerton JW, Stoodley P.** 2004. Bacterial biofilms: from the
529 natural environment to infectious diseases. Nat Rev Microbiol **2**:95–108.
530 2. **Flemming H-C, Wingender J, Szewzyk U, Steinberg P, Rice SA, Kjelleberg S.**
531 2016. Biofilms: an emergent form of bacterial life. Nat Rev Microbiol **14**:563–575.
532 3. **West SA, Diggle SP, Buckling A, Gardner A, Griffin AS.** 2007. The social lives
533 of microbes. Annu Rev Ecol Evol Syst **38**:53–77.
534 4. **Stewart PS, Franklin MJ.** 2008. Physiological heterogeneity in biofilms. Nat Rev
535 Microbiol **6**:199–210.
536 5. **Miquel S, Lagrafeuille R, Souweine B, Forestier C.** 2016. Anti-biofilm activity as
537 a health issue. Front Microbiol **7**:592. doi: 10.3389/fmicb.2016.00592
538 6. **Bjarnsholt T, Alhede M, Alhede M, Eickhardt-Sørensen SR, Moser C, Kühl M,**
539 **Jensen PØ, Høiby N.** 2013. The *in vivo* biofilm. Trends Microbiol **21**:466–474.
540 7. **Valderrama WB, Cutter CN.** 2013. An ecological perspective of *Listeria*
541 *monocytogenes* biofilms in food processing facilities. Crit Rev Food Sci Nutr
542 **53**:801–817.
543 8. **Mangwani N, Kumari S, Das S.** 2016. Bacterial biofilms and quorum sensing:
544 fidelity in bioremediation technology. Biotechnol Genet Eng Rev 8725. doi:
545 10.1080/02648725.2016.1196554
546 9. **Ramey BE, Koutsoudis M, Bodman SB Von, Fuqua C.** 2004. Biofilm formation
547 in plant-microbe associations. Curr Opin Microbiol **7**:602–609.
548 10. **Parsek MR, Greenberg EP.** 2005. Sociomicrobiology: the connections between
549 quorum sensing and biofilms. Trends Microbiol **13**:27–33.
550 11. **Mhatre E, Monterrosa RG, Kovács ÁT.** 2014. From environmental signals to

551 regulators: Modulation of biofilm development in Gram-positive bacteria. J Basic
552 Microbiol **54**:616–632.
553 12. **Espeso DR, Carpio A, Einarsson B.** 2015. Differential growth of wrinkled
554 biofilms. Phys Rev E **91**:22710. doi: 10.1080/02648725.2016.1196554
555 13. **Asally M, Kittisopikul M, Rué P, Du Y, Hu Z, Çağatay T, Robinson AB, Lu H,**
556 **Garcia-Ojalvo J, Süel GM.** 2012. Localized cell death focuses mechanical forces
557 during 3D patterning in a biofilm. Proc Natl Acad Sci U S A **109**:18891–18896.
558 14. **Wilking JN, Zaburdaev V, De Volder M, Losick R, Brenner MP, Weitz DA.**
559 2013. Liquid transport facilitated by channels in *Bacillus subtilis* biofilms. Proc Natl
560 Acad Sci U S A **110**:848–852.
561 15. **Vlamakis H, Chai Y, Beauregard P, Losick R, Kolter R.** 2013. Sticking together:
562 building a biofilm the *Bacillus subtilis way*. Nat Rev Microbiol **11**:157–168.
563 16. **Lopez D, Vlamakis H, Kolter R.** 2009. Generation of multiple cell types in
564 *Bacillus subtilis*. FEMS Microbiol Rev **33**:152–163.
565 17. **Mielich-Süss B, Lopez D.** 2015. Molecular mechanisms involved in *Bacillus*
566 *subtilis* biofilm formation. Environ Microbiol **17**:555–565.
567 18. **Bais HP, Fall R, Vivanco JM.** 2004. Biocontrol of *Bacillus subtilis* against
568 infection of Arabidopsis Roots by *Pseudomonas syringae* is facilitated by biofilm
569 formation and surfactin production. Plant Physiol **134**:307–319.
570 19. **Chen Y, Yan F, Chai Y, Liu H, Kolter R, Losick R, Guo JH.** 2013. Biocontrol of
571 tomato wilt disease by *Bacillus subtilis* isolates from natural environments
572 depends on conserved genes mediating biofilm formation. Environ Microbiol
573 **15**:848–864.
574 20. **Stein T.** 2005. *Bacillus subtilis* antibiotics: structures, syntheses and specific

575 functions. Mol Microbiol **56**:845–857.

576 21. **Todorova S, Kozhuharova L.** 2010. Characteristics and antimicrobial activity of
577 *Bacillus subtilis* strains isolated from soil. World J Microbiol Biotechnol **26**:1207–
578 1216.

579 22. **Fernandes PAV, De Arruda IR, Dos Santos AFAB, De Araújo AA, Maior AMS,**
580 **Ximenes EA.** 2007. Antimicrobial activity of surfactants produced by *Bacillus*
581 *subtilis* R14 against multidrug-resistant bacteria. Brazilian J Microbiol **38**:704–709.

582 23. **Shank EA, Klepac-Ceraj V, Collado-Torres L, Powers GE, Losick R, Kolter R.**
583 2011. Interspecies interactions that result in *Bacillus subtilis* forming biofilms are
584 mediated mainly by members of its own genus. Proc Natl Acad Sci U S A
585 **108**:E1236-1243.

586 24. **Bleich R, Watrous JD, Dorrestein PC, Bowers AA, Shank EA.** 2015.
587 Thiopeptide antibiotics stimulate biofilm formation in *Bacillus subtilis*. Proc Natl
588 Acad Sci U S A **112**:3086–3091.

589 25. **Powers MJ, Sanabria-Valentín E, Bowers AA, Shank EA.** 2015. Inhibition of cell
590 differentiation in *Bacillus subtilis* by *Pseudomonas protegens*. J Bacteriol
591 **197**:2129–2138.

592 26. **Roesch L, Fulthorpe R, Riva A, Casella G, Hadwin A, Kent A, Daroub S,**
593 **Camargo F, Farmerie W, Triplett E.** 2007. Pyrosequencing enumerates and
594 contrasts soil microbial diversity. ISME J **1**:283–290.

595 27. **Fierer N, Lennon JT.** 2011. The generation and maintenance of diversity in
596 microbial communities. Am J Bot **98**:439–448.

597 28. **Kraemer SA, Kassen R.** 2015. Patterns of local adaptation in space and time
598 among soil bacteria. Am Nat **185**:317–331.

599 29. **Algburi A, Comito N, Kashtanov D, Dicks LMT, Chikindas ML.** 2017. Control of
600 biofilm formation: antibiotics and beyond. Appl Environ Microbiol **83**:e02508-
601 02516.
602 30. **Sultana ST, Babauta JT, Beyenal H.** 2015. Electrochemical biofilm control: a
603 review. Biofouling **31**:745–758.
604 31. **Winkelströter LK, Teixeira FB dos R, Silva EP, Alves VF, De Martinis ECP.**
605 2014. Unraveling microbial biofilms of importance for food microbiology. Microb
606 Ecol **68**:35–46.
607 32. **Spiers AJ.** 2014. A mechanistic explanation linking adaptive mutation, niche
608 change, and fitness advantage for the wrinkly spreader. Int J Evol Biol
609 **2014**:675432. doi: 10.1155/2014/675432
610 33. **Gallegos-Monterrosa R, Mhatre E, Kovács ÁT.** 2016. Specific *Bacillus subtilis*
611 168 variants form biofilms on nutrient-rich medium. Microbiology **162**:1922–1932.
612 34. **Jiang M, Shao W, Perego M, Hoch JA.** 2000. Multiple histidine kinases regulate
613 entry into stationary phase and sporulation in *Bacillus subtilis*. Mol Microbiol
614 **38**:535–542.
615 35. **Vlamakis H, Aguilar C, Losick R, Kolter R.** 2008. Control of cell fate by the
616 formation of an architecturally complex bacterial community. Genes Dev **22**:945–
617 953.
618 36. **López D, Kolter R.** 2010. Extracellular signals that define distinct and coexisting
619 cell fates in *Bacillus subtilis*. FEMS Microbiol Rev **34**:134–149.
620 37. **Saxild HE, Nygaard P.** 1987. Genetic and physiological characterization of
621 *Bacillus subtilis* mutants resistant to purine analogs. J Bacteriol **169**:2977–2983.
622 38. **Murray AW.** 1971. The biological significance of purine salvage. Annu Rev

623 Biochem **40**:811–826.

624 39. **Dandanell G, Hove-Jensen B, Willemoës M, Jensen KF.** 2008. Nucleotides,
625 nucleosides, and nucleobases. EcoSal Plus 3. doi: 10.1128/ecosalplus.3.6.2

626 40. **Torres RJ, Prior C, Garcia MG, Puig JG.** 2016. A review of the implication of
627 hypoxanthine excess in the physiopathology of Lesch–Nyhan disease.
628 Nucleosides Nucleotides Nucleic Acids **35**:507–516.

629 41. **Kim Y-J, Ryu H-M, Choi J-Y, Cho J-H, Kim C-D, Park S-H, Kim Y-L.** 2017.
630 Hypoxanthine causes endothelial dysfunction through oxidative stress-induced
631 apoptosis. Biochem Biophys Res Commun **482**:821–827.

632 42. **Day RO, Kamel B, Kannangara DRW, Williams KM, Graham GG.** 2016.
633 Xanthine oxidoreductase and its inhibitors: relevance for gout. Clin Sci **130**:2167–
634 2180.

635 43. **Hill-Perkins M, Jones MD, Karran P.** 1986. Site-specific mutagenesis in vivo by
636 single methylated or deaminated purine bases. Mutat Res **162**:153–163.

637 44. **Ayala-García VM, Valenzuela-García LI, Setlow P, Pedraza-Reyes M.** 2016.
638 Aag hypoxanthine-DNA glycosylase is synthesized in the forespore compartment
639 and involved in counteracting the genotoxic and mutagenic effects of
640 hypoxanthine and alkylated bases in DNA during *Bacillus subtilis* sporulation. J
641 Bacteriol **198**:3345–3354.

642 45. **He M, Li X, Liu H, Miller SJ, Wang G, Rensing C.** 2011. Characterization and
643 genomic analysis of a highly chromate resistant and reducing bacterial strain
644 *Lysinibacillus fusiformis* ZC1. J Hazard Mater **185**:682–688.

645 46. **Zhao L, Bao G, Geng B, Song J, Li Y.** 2015. Draft genome sequence of
646 *Lysinibacillus fusiformis* strain SW-B9, a novel strain for biotransformation of

647 isoeugenol to vanillin. Genome Announc 3:e00289-15.
648 doi:10.1128/genomeA.00289-15
649 47. **Gupta S, Goyal R, Nirwan J, Cameotra SS, Tejoprakash N.** 2012.
650 Biosequestration, transformation, and volatilization of mercury by *Lysinibacillus*
651 *fusiformis* isolated from industrial effluent. J Microbiol Biotechnol **22**:684–689.
652 48. **Gallegos-Monterrosa R, Maróti G, Bálint B, Kovács ÁT.** 2016. Draft genome
653 sequence of the soil isolate *Lysinibacillus fusiformis* M5, a potential hypoxanthine
654 producer. Genome Announc 4:e01272-16. doi: 10.1128/genomeA.01272-16
655 49. **Wang S, Hu A.** 2016. Comparative study of spontaneous deamination of adenine
656 and cytosine in unbuffered aqueous solution at room temperature. Chem Phys
657 Lett **653**:207–211.
658 50. **Stefanic P, Decorosi F, Viti C, Petito J, Cohan FM, Mandic-Mulec I.** 2012. The
659 quorum sensing diversity within and between ecotypes of *Bacillus subtilis*. Environ
660 Microbiol **14**:1378–1389.
661 51. **Burmølle M, Ren D, Bjarnsholt T, Sørensen SJ.** 2014. Interactions in
662 multispecies biofilms: Do they actually matter? Trends Microbiol **22**:84–91.
663 52. **Kobayashi K.** 2007. *Bacillus subtilis* pellicle formation proceeds through
664 genetically defined morphological changes. J Bacteriol **189**:4920–4931.
665 53. **Kunst F, Rapoport G.** 1995. Salt stress is an environmental signal affecting
666 degradative enzyme synthesis in *Bacillus subtilis*. J Bacteriol **177**:2403–2407.
667 54. **Yan X, Yu H-JJ, Hong Q, Li S-PP.** 2008. Cre/lox system and PCR-based genome
668 engineering in *Bacillus subtilis*. Appl Environ Microbiol **74**:5556–5562.
669 55. **Devereux R, Wilkinson SS.** 2004. Amplification of ribosomal RNA sequences, p.
670 509–522. *In* Kowalchuk, GA, Bruijn, F de, Head, IM, Zijpp, AJ Van der, Elsas, JD

671 van (eds.), Molecular Microbial Ecology Manual, 2nd edition. Kluwer Academic
672 Publishers, Dordrecht, The Netherlands.
673 56. **Zhang Z, Schwartz S, Wagner L, Miller W.** 2000. A greedy algorithm for aligning
674 DNA sequences. J Comput Biol **7**:203–214.
675 57. **van Gestel J, Weissing FJ, Kuipers OP, Kovács ÁT.** 2014. Density of founder
676 cells affects spatial pattern formation and cooperation in *Bacillus subtilis* biofilms.
677 ISME J **8**:2069–2079.
678 58. **Perego M, Cole SP, Burbulys D, Trach K, Hoch JA.** 1989. Characterization of
679 the gene for a protein kinase which phosphorylates the sporulation-regulatory
680 proteins Spo0A and Spo0F of *Bacillus subtilis*. J Bacteriol **171**:6187–6196.
681 59. **Wang L, Grau R, Perego M, Hoch JA.** 1997. A novel histidine kinase inhibitor
682 regulating development in *Bacillus subtilis*. Genes Dev **11**:2569–2579.
683 60. **Grau RR, de Oña P, Kunert M, Leñini C, Gallegos-Monterrosa R, Mhatre E,**
684 **Vileta D, Donato V, Hölscher T, Boland W, Kuipers OP, Kovács ÁT.** 2015. A
685 duo of potassium-responsive histidine kinases govern the multicellular destiny of
686 *Bacillus subtilis*. MBio **6**:e00581-15. doi: 10.1128/mBio.00581-15
687 61. **López D, Fischbach MA, Chu F, Losick R, Kolter R.** 2009. Structurally diverse
688 natural products that cause potassium leakage trigger multicellularity in *Bacillus*
689 *subtilis*. Proc Natl Acad Sci U S A **106**:280–285.
690 62. **Koo B-M, Kritikos G, Farelli JD, Todor H, Tong K, Kimsey H, Wapinski I,**
691 **Galardini M, Cabal A, Peters JM, Hachmann A-B, Rudner DZ, Allen KN,**
692 **Typas A, Gross CA.** In press. Construction and analysis of two genome-scale
693 deletion libraries for *Bacillus subtilis*. Cell Syst. doi: 10.1016/j.cels.2016.12.013
694

695 63. **Murray EJ, Strauch MA, Stanley-Wall NR.** 2009. SigmaX is involved in
696 controlling *Bacillus subtilis* biofilm architecture through the AbrB homologue Abh. J
697 Bacteriol **191**:6822–6832.
698 64. **Casadaban MJ, Cohen SN.** 1980. Analysis of gene control signals by DNA fusion
699 and cloning in *Escherichia coli*. J Mol Biol **138**:179–207.
700 65. **Kovács ÁT, van Hartskamp M, Kuipers OP, van Kranenburg R.** 2010. Genetic
701 tool development for a new host for biotechnology, the thermotolerant bacterium
702 *Bacillus coagulans*. Appl Environ Microbiol **76**:4085–4088.
703

TABLES AND FIGURES

Table 1. Strains and plasmids used in this study.

Strain	Characteristics	Reference
B. subtilis		
168	168 1A700 *trpC*. Jena Stock	(33)
TB48	168 *trpC2 amyE*::$P_{hyperspank}$-*mKATE* (*cat*)	(57)
JH12638	JH642 *trpC2 phe*-1 *kinA*::Tn917(*cat*)	(58)
JH19980	JH642 *trpC2 phe*-1 *kinB*::*tet*	(59)
RGP0203-4	JH642 *kinC*::Sp^R	(60)
DL153	NCIB 3610 *kinD*::*tet*	(61)
BKE06370	168 *trpC2 pbuG*::Erm^R	(62)
BKE29990	168 *trpC2 pbuO*::Erm^R	(62)
NRS2243	NCIB 3610 *sacA*::P_{epsA}-*gfp* (*neo*), *hag::cat*	(63)
NRS2394	NCIB 3610 *sacA*::P_{tapA}-*gfp* (*neo*)	(63)
TB812	168 *trpC2 amyE*::$P_{hyperspank}$-*mKATE* (*cat*) *pbuG*::Erm^R	This study, BKE06370→TB48
TB813	168 *trpC2 amyE*::$P_{hyperspank}$-*mKATE* (*cat*) *pbuO*::Erm^R	This study, BKE29990→TB48
TB822	168 *trpC2 amyE*::$P_{hyperspank}$-*mKATE* (*cat*) Δ*pbuO*	This study
TB823	168 *trpC2 amyE*::$P_{hyperspank}$-*mKATE* (*cat*) Δ*pbuO, pbuG*::Erm^R	This study, BKE06370→TB822
TB833	168 *trpC2 amyE*::$P_{hyperspank}$-*mKATE* (*cat*) *kinA*::Tn917(*cat*)	This study, JH12638→TB48
TB834	168 *trpC2 amyE*::$P_{hyperspank}$-*mKATE* (*cat*) *kinB*::*tet*	This study, JH19980→TB48
TB835	168 *trpC2 amyE*::$P_{hyperspank}$-*mKATE* (*cat*) *kinC*::Sp^R	This study, RGP0203-4→TB48
TB836	168 *trpC2 amyE*::$P_{hyperspank}$-*mKATE* (*cat*) *kinD*::*tet*	This study, DL153→TB48
TB869	168 *trpC2 amyE*::$P_{hyperspank}$-*mKATE* (*cat*) *sacA*::P_{epsA}-*gfp* (*neo*)	This study, NRS2243→TB48
TB870	168 *trpC2 amyE*::$P_{hyperspank}$-*mKATE* (*cat*) *sacA*::P_{tapA}-*gfp* (*neo*)	This study, NRS2394→TB48
E. coli		
MC1061	Cloning host; K-12 F^- λ^- Δ(*ara-leu*)7697 [*araD*139]B/r Δ(*codB-lacI*)3 *galK16 galE15* $e14^-$ *mcrA0 relA1 rpsL150*(Str^R) *spoT1 mcrB1 hsdR2*(r^- m^+)	(64)

Soil Isolates		
Lysinibacillus sp. M2c		This study
Lysinibacillus fusiformis M5		This study
Bacillus pumilus P22a		This study
Acinetobacter variabilis T7a		This study
Plasmid	**Characteristics**	**Reference**
pMH66	pNZ124-based Cre-encoding plasmid, Tet^R Ts	(65)

Table 2. PCR primers used in this study.

Primer	**Sequence (5´ → 3´)**	**Target locus**
oGFPrev2	TTGTGCCCATTAACATCACC	*gfp*
oRGM110	GGAATCCGCGCCGTTACATC	*pbuG*
oRGM111	CAGCCCATATAGCAAAGACC	*pbuG*
oRGM116	GCGGTGCGGAATAAGTAAAG	*pbuO*
oRGM117	TACTGAGCGGCACTTGCTTG	*pbuO*
oRGM130	TATCCACGCCTACGCAGAGC	*kinA*
oRGM131	CTCAATGGACACGCTGAGAG	*kinA*
oRGM132	GAAGACCAGCAAGCAAATCG	*kinD*
oRGM133	GCGGCTGATCGCCTTTATGG	*kinD*
oRGM38	GAGAATTCGTGGTGCCAAAGACGAGAAG	*tapA* promotor
oRGM40	GAGAATTCCCAGCTGATTAATAGAATAG	*epsA* promotor
oTB55	CATGGGATCCTGGCGGAGAAGGATTTATG	*kinB*
oTB56	CACGGAATTCTGTCTCAAACGTGCTCATC	*kinB*
oTB61	CATGGGATCCATTACGCTAAGCCCTGAG	*kinC*
oTB62	CACGGAATTCTTGTGCCAGCAAATGATG	*kinC*
27F	AGAGTTTGATCMTGGCTCAG	16S rRNA
1492R	TACGGYTACCTTGTTACGACTT	16S rRNA

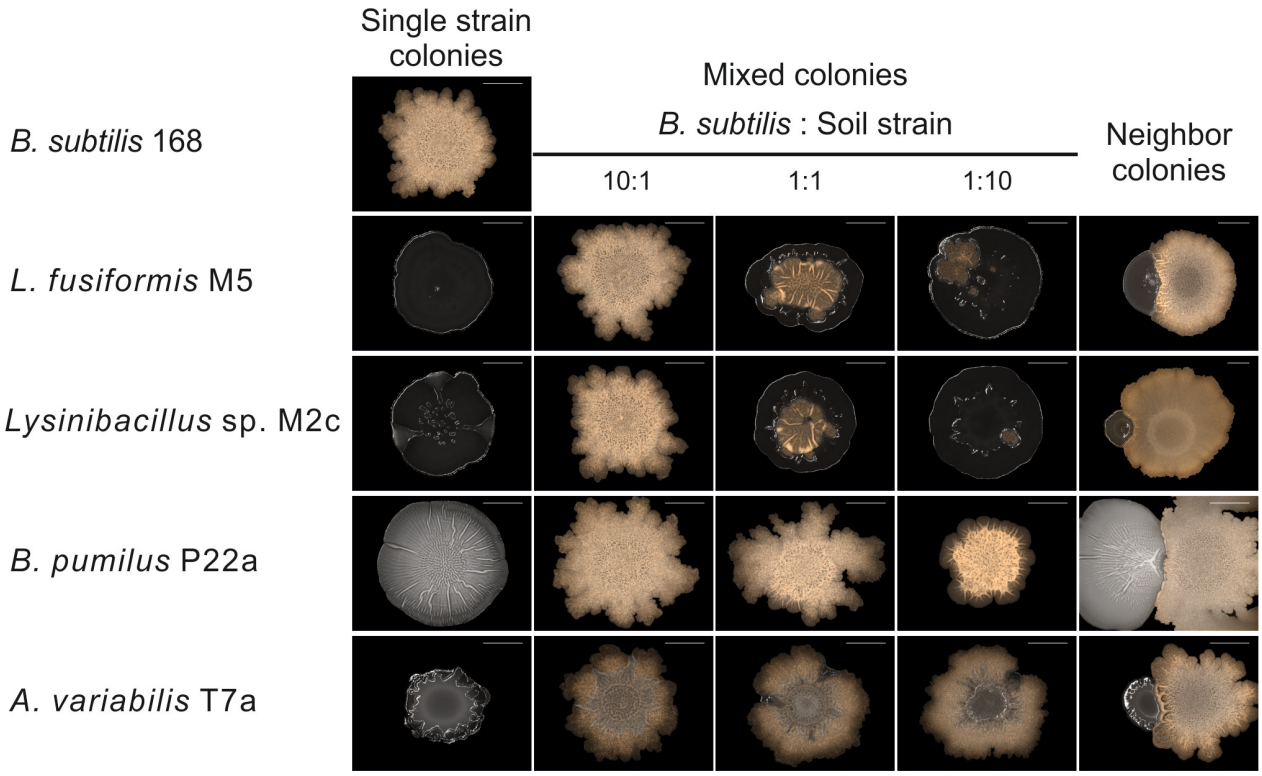

Figure 1. Single strain and mixed colonies of *B. subtilis* and selected soil strains. *B. subtilis* was differentiated from the soil strains using fluorescence emission (false-colored orange) from a reporter expressed by the $P_{hyperspank}$-mKATE construct. Neighbor colonies were inoculated with 2 μL of cultures at 5 mm from each other. Scale bars represent 5 mm.

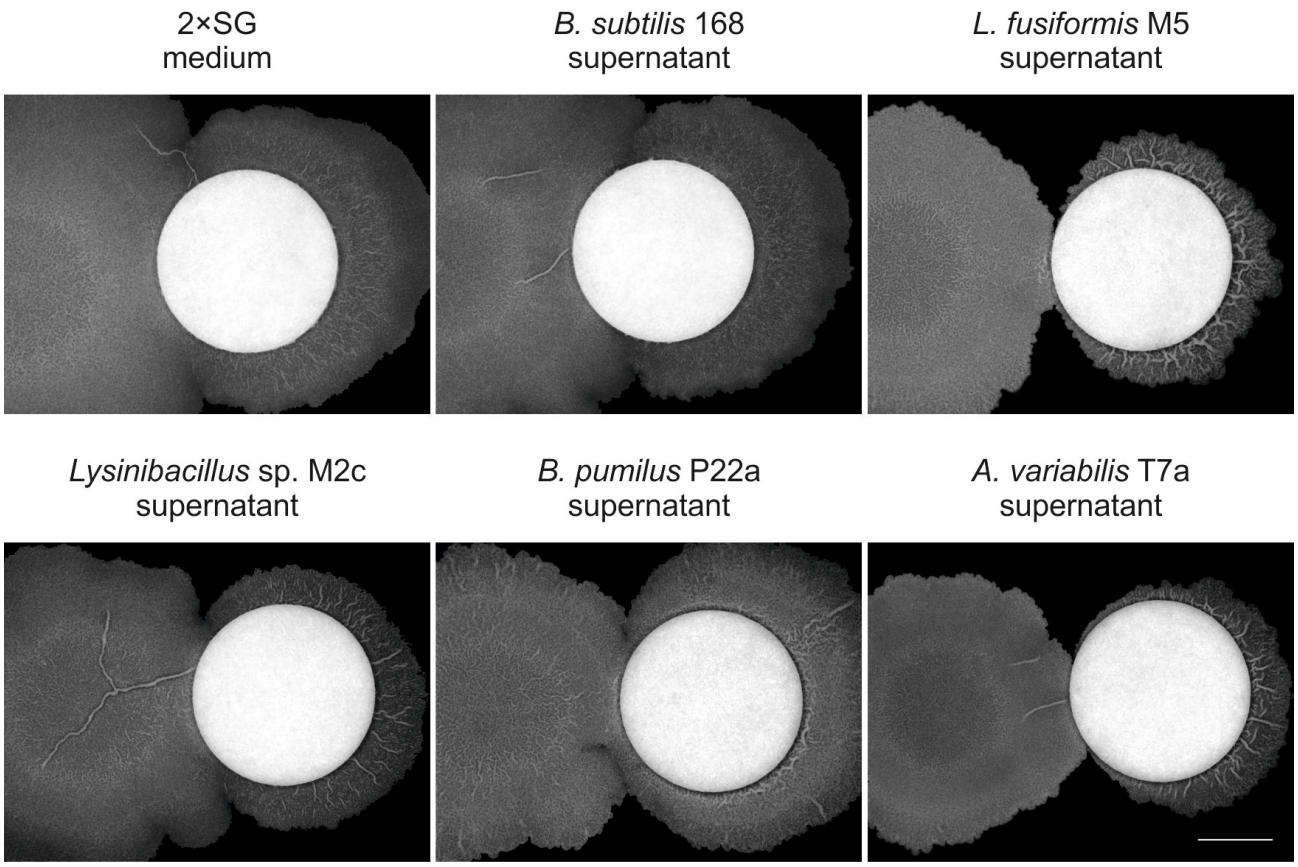

Figure 2. Effect of cell-free supernatants of soil strains on the development of *B. subtilis* 168 biofilm colonies. Bright-field images of colonies are shown. The scale bar represents 5 mm.

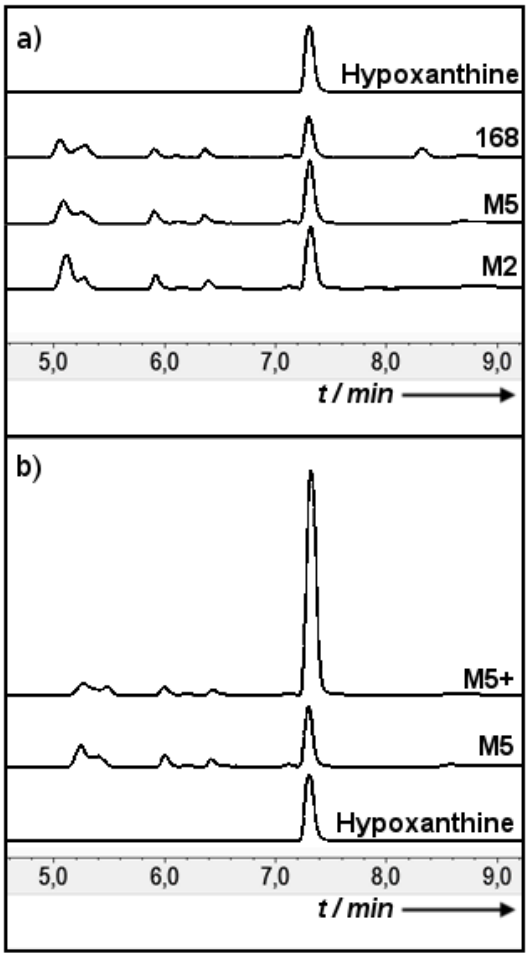

Figure 3. Characterization of hypoxanthine standard and cell-free supernatants of *B. subtilis* 168 (168), and soil isolates *L. fusiformis* M5 (M5) and *Lysinibacillus* sp. M2c (M2). a) HPLC chromatograms of cell-free supernatants compared to a standard solution of hypoxanthine. b) HPLC chromatogram of *L. fusiformis* M5 cell-free supernatant compared with a standard solution of hypoxanthine, and the *L. fusiformis* M5 cell-free supernatant spiked with a standard of hypoxanthine (M5+).

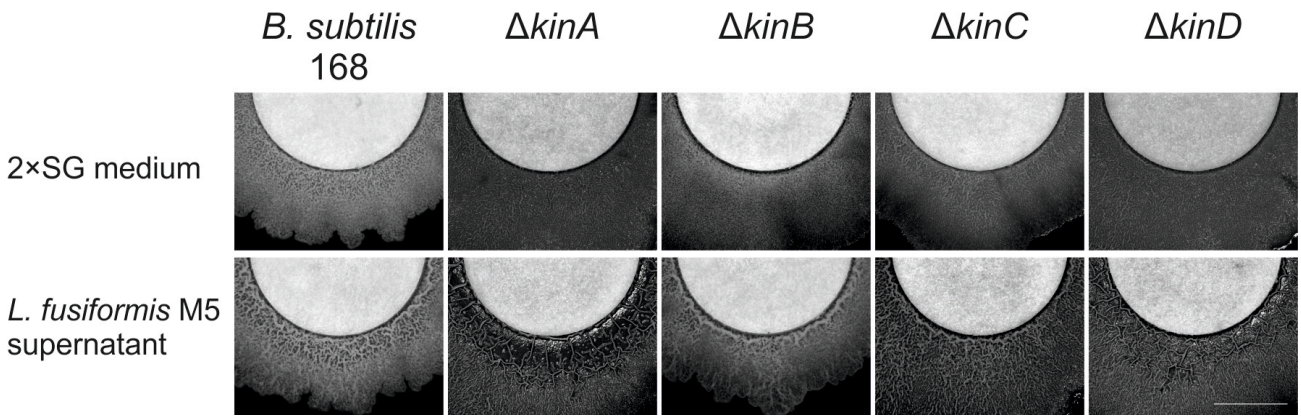

Figure 4. Effect of cell-free supernatant of *L. fusiformis* M5 on the development of biofilm colonies of *B. subtilis* 168 and knock-out mutants of kin-kinase genes. Bright-field images of colonies are shown. The scale bar represents 5 mm.

B. subtilis TB869 (P_{epsA}-*gfp*, $P_{hyperspank}$-*mKATE*)

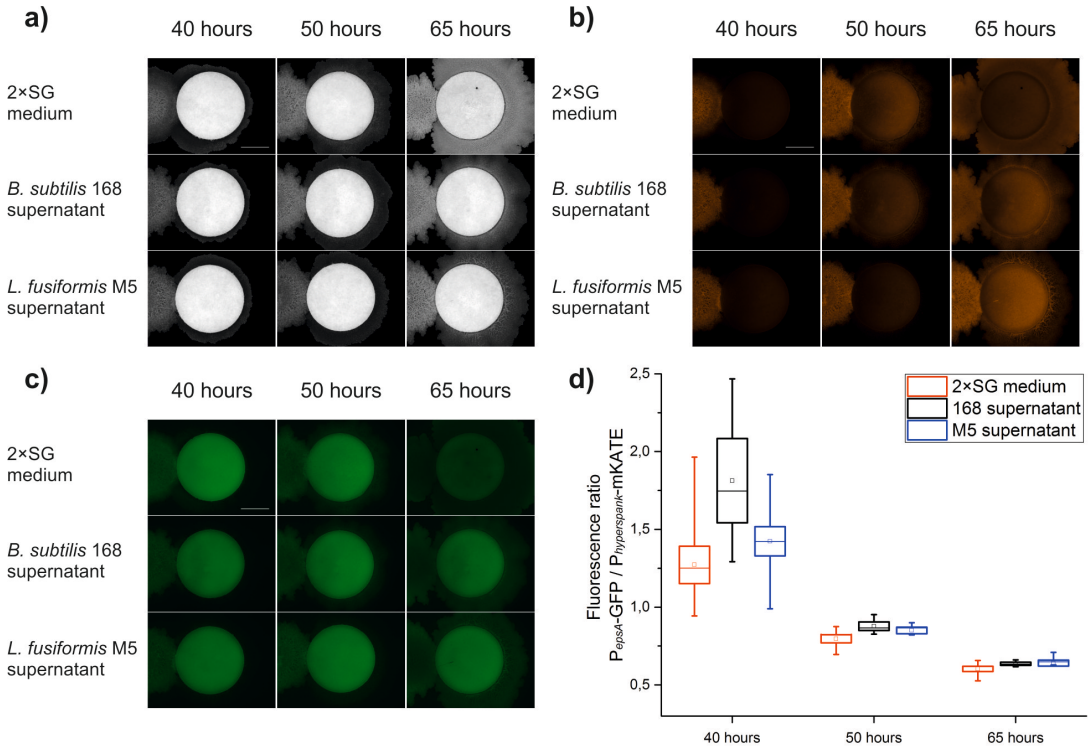

B. subtilis TB870 (P_{tapA}-*gfp*, $P_{hyperspank}$-*mKATE*)

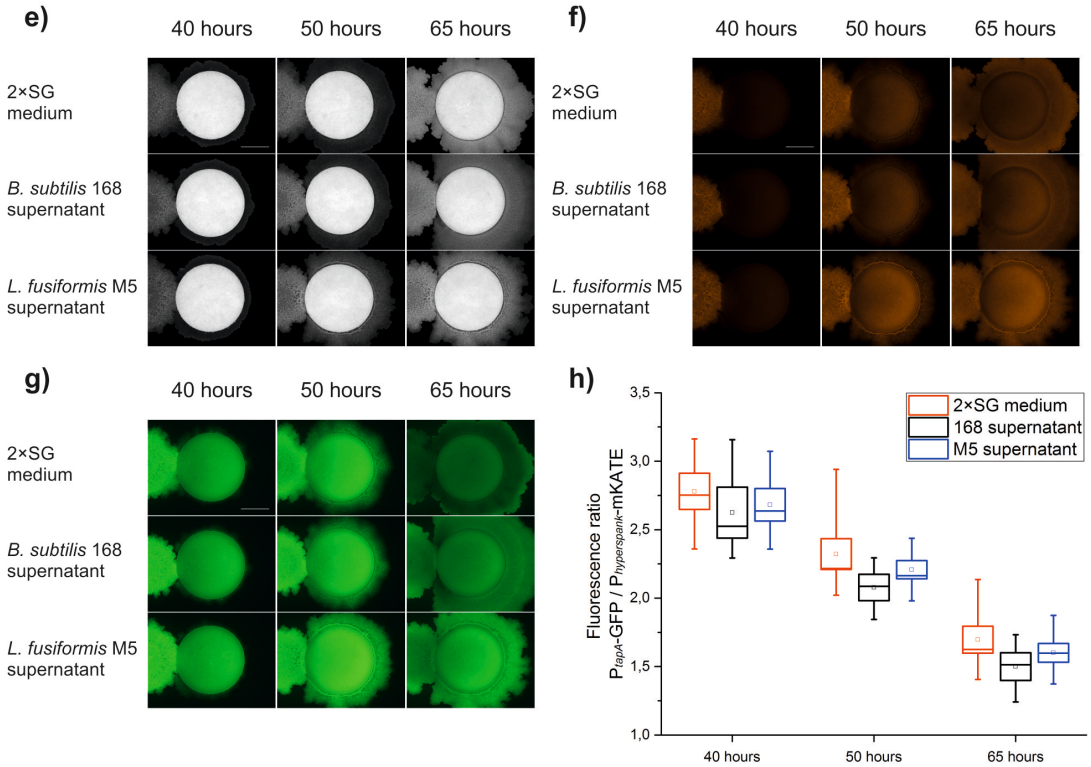

Figure 5. Comparison of fluorescence emission of *B. subtilis* strains carrying the constitutive $P_{hyperspank}$-*mKATE*, and the P_{epsA}-*gfp* (a-d) or P_{tapA}-*gfp* (e-h), reporter fusions. Bright field (a and e), red fluorescence (b and f), and green fluorescence images (c and g) of representative *B. subtilis* biofilm colonies exposed to cell-free supernatants of *B. subtilis* 168, *L. fusiformis* M5 and 2×SG medium. Box plots on the ratio of green and red fluorescence emission of biofilm colonies of *B. subtilis* TB869 (d) and TB870 (h) exposed to cell-free supernatants of *B. subtilis* 168, *L. fusiformis* M5 and 2×SG medium at different time points. Scale bars represent 5 mm. Box plots (d and h) represent fluorescence ratios of at least 4 independent colonies, processed as described in material and methods. (one-way ANOVA: $P<0.05$, n=4-8 independent colonies).

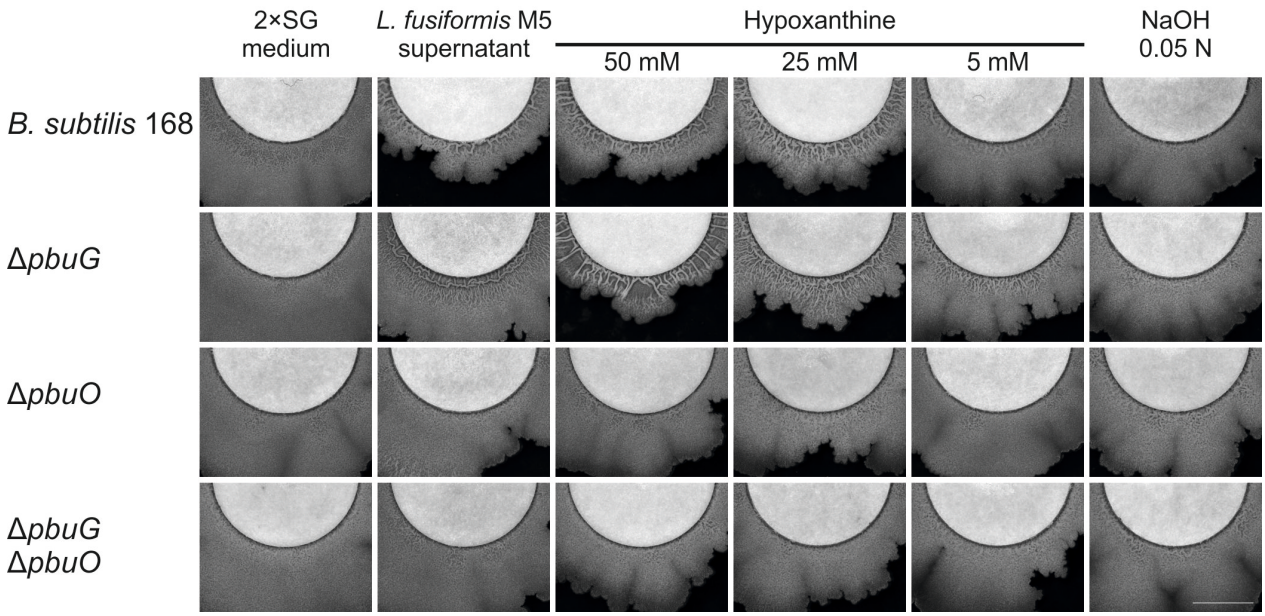

Figure 6. Effect of hypoxanthine and cell-free supernatant of *L. fusiformis* M5 on the development of biofilm colonies of *B. subtilis* 168 and knock-out mutants of *pbuO* and *pbuG* permease genes. Bright-field images of colonies are shown. The scale bar represents 5 mm.